quantum beam science

MDPI

Article

New Structural Insight into Interface-Controlled α–σ Phase Transformation in Fe-Cr Alloys

Wael Al Khoury [1], Nobumichi Tamura [2], Guillaume Geandier [3] and Philippe Goudeau [4,*]

1 Atomic Energy Commission of Syria (AECS), P. O. Box 6091, Damascus, Syria; walkhoury@aec.org.sy
2 ALS–LBNL, 1 Cyclotron Road, MS 2-400, Berkeley, CA 94720, USA; ntamura@lbl.gov
3 Institut Jean Lamour, UMR 7198 CNRS Université de Lorraine, Campus Artem, 2 Allée André Guinier, BP 50840, 54011 Nancy CEDEX, France; guillaume.geandier@univ-lorraine.fr
4 Institut Pprime, UPR 3346 CNRS—Université de Poitiers-ENSMA, SP2MI, Boulevard Marie et Pierre Curie, BP30179, 86962 Futuroscope, France
* Correspondence: philippe.goudeau@cnrs.pprime.fr; Tel. +33-5-49-49-67-26

Received: 31 October 2018; Accepted: 30 November 2018; Published: 10 December 2018

Abstract: Synchrotron Laue microdiffraction scanning is used for the ex situ study of the body-centered, cubic-to-tetragonal phase transformation that occurs in equiatomic polycrystalline Fe-Cr alloys at temperatures between 550 and 800 °C. Grain orientation and grain strains were scanned with a micron step resolution after annealing at 700 °C for 12 h. Further microstructural details on the early stage of the transformation, and more particularly on the cubic-to-tetragonal phase interface, were achieved. Only the α and ordered σ phases were detected. The crystallographic relationships at the interface between the two phases did not follow the predicted rules; this result is discussed in relation to the measured microstrains.

Keywords: synchrotron X-ray diffraction; iron alloys; phase transformations; grain orientation; grain/phase boundaries; strain/stress measurement

1. Introduction

Body-centered cubic (bcc) Fe-Cr solid solutions undergo a phase transformation into a complex tetragonal sigma phase with equiatomic composition at temperatures between 550 and 800 °C. Although this phase was detected 85 years ago by Bain et al. [1], and its complete structure was solved only 30 years later by Bergman et al. [2] using X-ray diffraction, the origin and mechanisms of the transformation process are still debated now by theoreticians and experimentalists. More precisely, extensive works have studied (1) the existence of an intermediate phase that has a cubic B2 structure, and thus a tendency to: ordering prior transformation; (2) crystallographic relationships between the two phases; and (3) the distribution of alloy constituents on the different atomic sites. In spite of these numerous simulations and experimental studies, no clear answers have been given, and most of these questions remain unanswered because of a lack of experimental work with submicron scales. The original work accomplished in this paper, thanks to the powerful micro Laue diffraction technique, fills in this gap and contributes to the understanding of the phase transformation from a simple cubic structure to a more complex Franck Kasper (FK) structure. The study of these complex structures is of fundamental interest because they display structural units that are believed to be present in nonperiodic systems. Furthermore, the brittle σ-phase appears as a precipitate during steel production, therefore, since it may deteriorate the mechanical and corrosion properties in such alloys, this is of technological interest for nuclear applications [3–5].

Mössbauer's investigations of the magnetic and structural properties of the α-to-σ phase transformation in equiatomic Fe-Cr alloys, led Dubiel and coworkers [6] to adopt the idea previously raised by Kitchingman [7] of an intermediate phase with a B2 ordered cubic structure. According to

Kitchingman [7], atomic movements over small distances in the <11–1> direction take place, leading to the formation of a new layer structure. The transformation is completed by the rotation of the alternate layers of hexagons, within zones related to Kagome title structures. This mechanism suggests that certain groups of atoms are more strongly bonded in the 11–1 direction than others, and also that the bcc phase exhibits a partial long range order, prior to the transformation. At the same time, the short range order (SRO) in Fe-Cr alloys was investigated by X-ray scattering, but the authors were not able to detect any premonitory signatures of the σ–phase [8]. Other Fe-based intermetallic alloys, such as Fe-V, also show the same α-to-σ transition, however with significant differences concerning the temperature range of the transformation, the atomic distributions on the different sites of the complex structure, and finally, the tendency for ordering or phase separation existing in the parent bcc alloy. Indeed, it is now well established that FK phases satisfy Goldschmidt–Hume-Rothery rule that suggests that their formation is electronically driven. The Hume-Rothery rules for alloy structures cite the atomic size mismatch and the electron concentration per atom as the relevant variables, which may explain the different behaviors observed in Fe-V and Fe-Cr alloys. Indeed, the size difference between pure Cr and Fe was only 0.06%, which is one of the smaller differences in binary metallic solutions. In a first-principles study of the stability and local ordering of substitutional alloys, Turchi et al. [9] showed that Fe-Cr exhibits an overall tendency toward phase separation, whereas Fe-V has a definite tendency towards ordering, with a B2 superstructure of the CsCl type. However, strong tendencies towards order or phase separation would be energetically too costly to form a σ nucleus in the early stage of the nucleation, of the σ phase in the bulk bcc-based alloy, where important atomic displacements from the bcc lattice positions are required. Meanwhile, it has been experimentally observed in such alloys that the formation of the σ product preferentially initiates in the vicinity of the free surface or grain boundaries in polycrystalline materials of the bcc parent phase [10,11]. Hence, the phenomena pertaining to surfaces and interface boundaries (reconstruction, segregation, excess volume, etc.) should exhibit similar features for both alloys, in clear contrast to the bulk properties, as shown before. Therefore, it appears that SRO is not a major precursor for the nucleation of the σ phase, and the transformation mechanisms at the interface between the two phases remains poorly understood. In a recent work based on transmission electron microscopy, Ustinovshikov et al. [12] shown that the B2 ordered phase is not evidenced in equiatomic FeV alloys, contrary to simulation predictions. This feature has not yet been experimentally evidenced for the Fe-Cr system.

The α-to-σ phase transformation is a massive first-order transformation. In interface-controlled solid state transformations, the processes at the interface determine the transformation rate [13]. In particular, the amount of excess volume associated with an interface boundary and its distribution along the interface (which depends on the crystallography of the interface), control the activation enthalpies of interface mobility and boundary self-diffusion. Any excess volume at a boundary is caused by the misfit of the atoms of the two different crystals at the boundary, and its amount depends on the interface structure. Interface mobility and its orientation dependence are related to the misfit at the interface. A highly disordered boundary can be expected to have a large amount of excess volume, and increased excess volume leads to higher interface mobility and faster diffusion. During the phase transformation, vacancies are formed at the interface by fluctuations in the distribution of the excess volume at the interface. Atoms at the interface can take intermediate, energetically more favorable positions compared to positions at the ideal (bulk) lattice sites, thereby relaxing the interface structure. When coherence occurs at interfaces, there is almost no free space available for the movement of the atoms. Increasing the random site density at the interface leads to two opposite effects (freedom of movement of atoms and enhanced relaxation) on interface mobility activation energy, where the net result depends on the crystallography of the interface. To summarize the different steps of the transformation, the reaction is proceeded by the nucleation and growth mechanism, with a weak nucleation site density, and fast growth. Two successive steps have to be considered in polycrystalline and single crystal materials: (i) σ phase nuclei or germs are formed along initial grain boundaries, or free surfaces of the α phase, and then (ii) α grains grow inward. The limiting reaction takes place at

the internal interface between the grain and the nuclei. The nucleation is the process wherein spots (called nuclei or germs) appear in space and time, assumed to be a stochastic process. The growth process is deterministic and spatially homogeneous [14]. Due to the crystallographic complexity of the σ phase, the grain size, and sometimes the presence of an additional third element, the transformation process may be very slow [15].

2. Materials and Methods

The crystal structure of the σ-phase is tetragonal, with the lattice constants a_0 = 0.87995 nm and c_0 = 0.45442 nm [16]. Its space group is P42/mnm, and the corresponding Pearson symbol is tP30. The unit cell of the sigma phase contains 30 atoms that pertain to the five crystallographically-inequivalent sites A, B, C, D, and E, with the occupation numbers 2, 4, 8, 8, and 8, respectively. Three types of coordination occur: the A and D sites are icosahedrally coordinated, the B site has 15 near neighbors, and the C and E sites are 14-fold coordinated [2]. Concerning the atomic distribution on the sites, a discrepancy existed between the simulation and instrumental experiments, with the first stating that Fe occupies only three of the five places [17], whereas the second showed the presence of Fe on all five sites, but with a nonstatistical distribution [18]. A recent theoretical work was able to reproduce the experimentally observed site occupancy in the Fe-Cr sigma-phase [19] and furthermore, neutron diffraction studies [20] have confirmed that all five crystallographic sites in the σ-phase of Fe-Cr and Fe-V systems are mixed, that is, occupied by both kinds of alloy constituting elements. However, actual site-occupancy numbers are characteristic of the system, and are strongly influenced by the preparation conditions of the samples. The distribution of elements over the sites is not random, sites A and D are predominantly occupied by Fe, while sites B, C, and E are predominantly occupied by Cr or V atoms.

White beam Laue diffraction has never been used before to study the σ phase structure, and more particularly in the case of Fe-Cr alloys, whereas some structural studies have been done at synchrotron radiation facilities (SR) to maximize the scattering contrast between Fe and Cr. Yakel et al. [18] derived accurate site occupation parameters from SR diffraction data, recorded at the Stanford Synchrotron Radiation Laboratory (SSRL; USA). More recently, Reinhard et al. [8] also achieved anomalous measurements at the National Synchrotron Light Source (NSLS; USA) to enhance the contribution of SRO scattering. The bcc B2 ordered structure, prior to σ-phase transformation, is difficult to evidence with X-rays in Fe-Cr alloys, since the atomic scattering contrast between iron and chromium atoms is small and the satellite peak intensities are weak. The calculated intensity ratio between satellite peaks and the more intense X-ray diffraction peaks is about 0.1%, and thus conventional X-ray diffraction (XRD) tools are not able to reveal such low diffracted intensities. On the contrary, Laue diffraction performed on a single crystal with a white beam, provided by a very intense X-ray source available at new generation synchrotron facilities and recorded with a two dimensional detector, may be sensitive to such weak signals. Furthermore, using focusing optics and an X-Y sample stage, we were able to scan the interface crystallography between the two phases as well as the elastic and plastic strains at a submicron scale.

Disk-shaped samples, between 0.8–1.0 mm thick, were cut from a Fe-Cr rod material furnished by a steel factory (Imphy, France). The surface was then mechanically polished following a very strict procedure, developed by the polishing machine manufacturer Struers Inc. (Cleveland, OH, USA) for steel samples. The quality of the surface led to an rough mean squared roughness of around 0.5 nm. After a homogenization treatment at 1000 °C for 1 h in sealed quartz tube under a secondary vacuum, the samples were then annealed at 700 °C for 12 h and quenched in air. The average grain size in the alpha phase was estimated to be 100 µm using metallographic measurements with an optical microscope. In such an analysis, grain boundaries are revealed using chemical etching using the acid mixture called aqua regia, comprising 1 volume of HNO3 for every 3 volumes of HCl. Owing to the large grain size, the bcc-σ transformation is then very sluggish, and thus the annealing time corresponds to the early stage of transformation [21]. It is important to note that such a quench preserves the high temperature equilibrium configurational order [8]. The chemical composition was measured using energy X-ray dispersive (EDX) analyses in a scanning electron microscope (SEM), after homogenization, and also annealing treatments.

The Cr concentration as determined by EDX–SEM was 47.0% Cr, with a homogeneity of about 0.1% over the irradiated sample volume in the XRD experiment. The same results were obtained for Cr concentrations, whatever the treatment and the investigated phases. Because an absorption contrast exists for electrons between the two phases (the σ phase is dense), it was possible to image the two phases using SEM. Figure 1 shows the early stage of the phase transformation occurring in the sample; the grain boundaries of the initial α phase are also clearly visible. Microcracks due to volume variations were presents in the σ regions (white) and the distribution of this new phase shown in that image clearly indicates a nucleation process at grain boundaries, which then propagates inside the α grains. This verifies the description given in the previous paragraphs.

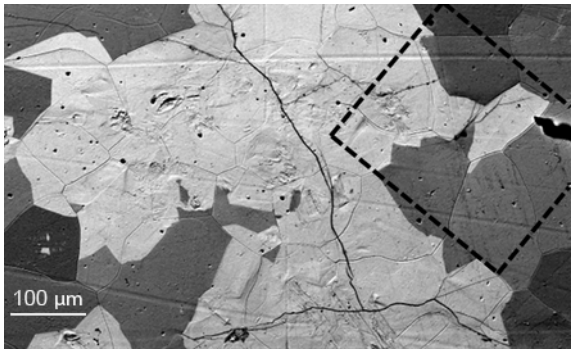

Figure 1. Scanning electron microscope (SEM) image in Backscattered electron shadow (BES) mode of the sample surface where the σ-phase is clearly visible (white) with the α-phase (grey). The dashed line delimits the scanned area during micro X-ray diffraction (XRD) measurements.

Scanning X-ray micro diffraction experiments were performed at the microdiffraction beamline (7.3.3, then moved to 12.3.2 for upgrade) of the Advanced Light Source (ALS; USA). The essential features of the beam optics are a Kirkpatrick-Baez (KB)'s focusing element, which allowed us to obtain a submicron spot at the sample surface, and a monochromator for switching between white and monochromatic beams, while keeping the beam position at the sample surface. The sample was mounted on a X-Y sample stage for scanning measurements, and the two-dimensional diffraction patterns were recorded thanks to a MAR CCD camera from marUSA, Inc. (Fairfield, NJ, USA). This beam line has been described in detail elsewhere [22]. We used the software named XMAS, developed at the beam line by Tamura, to analyze the XRD data obtained using the reflection diffracting configuration [23]. The analysis of the Laue diffraction patterns yielded the grain orientation maps of both phases, as well as deviatoric strain and dislocation density maps. One limitation in the use of polychromatic radiation to measure strains is that the dilatational component is not accessible using this method. Indeed, the wavelength of some reflections must be measured. Switching between white and monochromatic radiation allows for such measurement. However, the complete determination of the strain tensor in the Fe-Cr system needs to measure a large number of reflections, due to the presence of a strong elastic anisotropy. These measurements, which are time consuming, were not carried out in this study.

The different Laue patterns were indexed either with the bcc α-phase, or the tetragonal σ-phase structures. No substructure diffraction peaks related to the B2 ordered phase were detected, whereas diffraction peaks of the σ-phase, which had similar calculated intensities, were indexed. A sample that was totally σ transformed after annealing at 700 °C for 48 h was measured, and the obtained Laue patterns for different σ grain orientations were similar to the ones measured on the partially transformed sample. Up to one hundred Laue spots, revealing the complexity and the symmetry of the structure were indexed, which indicates the good quality of the acquired XRD data and the capability of the software. The c/a ratio that was found (0.5185) was slightly larger than the one previously reported in the literature (0.5164) [16]. This may be due to the sample elaboration and preparation conditions, as well as its exact chromium composition (47.0% in our study compared to 49.5% Cr in reference [16]).

3. Results and Discussion

Figure 2 shows the results obtained for a large scan of 405 × 405 µm, with a step of 5 µm and a beam size smaller than 1 µm. The recording time was 3 s per point, which resulted in a total scan time of 6 h. The insert shows deviatoric stresses in the α phase (the σ elastic constants are not known), corresponding to a 304 × 304 µm scan with a step size of 4 µm. The recording time per point was 4 s, which led to a scan duration of 7 h. We were not able to find rational crystallographic relationships between the two α and σ phases, contrary to the predicted rules of Kitchingman [7]: $[0,0,1]_\sigma // [1,1,\bar{1}]_\alpha$, $[\bar{1},\bar{4},0]_\sigma // [1,\bar{1},0]_\alpha$.

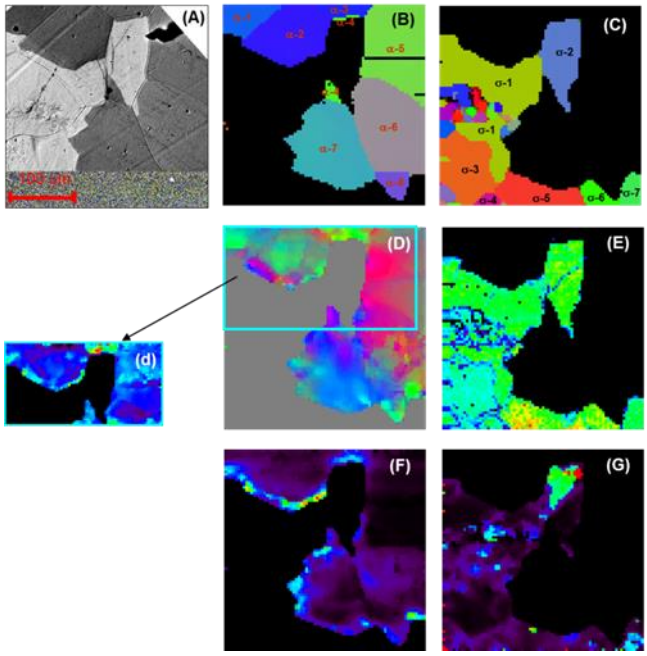

Figure 2. (Color online) Micro X-ray diffraction scanning of the sample surface as shown on the SEM image (**A**). (**B**,**C**) are the corresponding crystalline orientation maps, represented in the RGB system (Red: (001), Green: (011) and Blue: (111)) for the α and σ phases respectively. (**D**,**E**) are deviatoric strain maps, also represented in the RGB, system with the following correspondence for directions R: xx, G: yy et B: zz for α and σ phases respectively; Insert (**d**) shows the stress map for the α phase corresponding to a smaller area on the sample surface. (**F**,**G**) are the Laue spot broadening maps (related to dislocation densities) for the α and σ phases respectively.

In Figure 2B,C, grains were indexed in both phases according to their crystalline orientation. Determining the conversion matrix between two adjacent grains, such as tetragonal σ-2 and its parent cubic α-4, or tetragonal σ-5 and its parent cubic α-7, we obtained:

$$[1,0,0]_T // \sim [0,2,1]_C$$
$$[0,1,0]_T // \sim [\bar{2},\bar{1},2]_C$$
$$[0,0,1]_T // \sim [2,\bar{1},2]_C$$

and

$$[1,0,0]_T // \sim [2,\bar{1},3]_C$$
$$[0,1,0]_T // \sim [3,\bar{1},2]_C$$
$$[0,0,1]_T // \sim [0,3,1]_C$$

respectively.

Thus, there was no rational relationship between the crystallographic orientations of the parent α phase and the resulting σ phase. This was checked for other regions in the sample. The interfaces

were very disordered, as was revealed by the peak width mapping in both phases (see Table 1). The peak broadening was related to microstrains, which revealed the presence of extended defects such as dislocations and grain boundaries, punctual defects, and distortions of the unit cell, due to the cubic-to-tetragonal transformation.

The macrodeviatoric strains were relatively weak and uniform inside the grains, with a strong variation at the grain boundaries (see Table 1). This is in agreement with the stress relaxation generated by the appearance of microcracks in the σ phase (Figure 1). We observed growing of the σ phase from one boundary of a parent α phase, and its propagation through the adjacent grain, keeping the initial crystallographic orientation. In addition, the small σ grain set revealed in Figure 2C, related to the surface defects visible in Figure 2A, probably indicates that the σ phase nucleation arose close to these defects.

This behavior was totally different to that which was observed in a commercial 2205 duplex stainless steel by transmission electron microscopy [24]. The authors found a rational orientation relationship between the σ precipitate and parent δ ferrite (bcc). The parallel relationship between the planes of (–110)σ and (1–10)δ was revealed in the diffraction pattern. The interplanar spacing of (–110)σ was approximately three times (exactly 3.079 times) that of (1–10)δ, favoring the orientation relationship between the σ phase and δ ferrite, (–110)σ//(1–10)δ, [332]σ//[–1–1–3]δ; or expressed as (–3–1–2)σ//(211)δ, [–1–12]σ//[–1–13]δ. The relationship may be responsible for the pyramid morphology of the σ phase observed in the initial stage of precipitation. The particular microstructure of this alloy—the presence of the face-centered cubic (fcc) phase, carbide precipitates, and additional elements such as Ni and Mo—could explain the observed differences. For instance, the increase in the lattice constant of the σ phase was presumably due to the addition of the interstitial atom N, and the larger substitutional atoms Mo and Ni, as well as the higher Fe/Cr atomic ratio in the duplex stainless steel.

Table 1. In-grain strains (min, max) and peak broadening (min, max) in alpha and sigma phases extracted from Laue patterns. Uxx, Uyy, and Uzz are the macrostrains corresponding to the (001), (011), and (111) directions respectively (see Figure 2). Peak broadening W is given for grains indexed with at least seven Laue spots.

Fe-Cr	α	σ
Uxx (%)	(−2.0, +1.5)	(−4.2, 0.0)
Uyy (%)	(−4.0, +2.0)	(−3.2, +2.4)
Uzz (%)	(−2.5, +3.0)	(−0.6, +5.0)
W (°)	(0.07, 0.20)	(0.10, 0.20)

4. Conclusions

Imaging structural distortions (microstructures) related to phase transformation through scanning micro X-ray diffraction, provides new insight concerning the α-to-σ phase transition in Fe-Cr systems. The formation of the σ phase takes place predominantly along the grain boundaries, while reversal transformation takes place in the whole volume of the sample [25]. Thus, the σ phase transformation is grain size dependent. We did not find evidence of an intermediate phase during the transformation process, nor rational crystallographic relationships between the σ phase and its parent α phase.

This pioneering experimental work calls into question previous theoretical works related to the crystallographic changes accompanying this complex phase transformation. However, a more complete description of the phenomenon is necessary to confirm these first results. This should be based on: (1) electron backscatter diffraction (EBSD) in a SEM investigation of grain orientation that is more sample surface sensitive (i.e., 0.2 μm probed in depth compared to the 5 to 10 μm possible with X-rays); and (2) a micro XRD on a sample cross-section and transmission electron microscopy (TEM) investigation, for information on the bulk of the sample grains. Finally, the kinetics of this process are slow enough to allow in-situ measurements when the grain size is relatively large, thanks to the upgraded beam line at ALS [26], or more recently at the European synchrotron radiation facility (ESRF;

Grenoble, France) [27]. These provide faster and more accurate measurements owing to the more intense and smaller beam.

Author Contributions: Conceptualization, P.G.; software, N.T.; formal analysis, W.A.K.; investigation, G.G.; writing—original draft preparation, P.G.; writing—review and editing, N.T.

Funding: We are appreciative for access to the microdiffraction beamline of the Advanced Light Source (ALS). ALS is supported by the Director, Office of Science, Office of Basic Energy Sciences, Materials Sciences Division, of the U.S. Department of Energy under Contract DE-AC02-05CH11231 at Lawrence Berkeley National Laboratory and the University of California, Berkeley.

Conflicts of Interest: The authors declare no conflicts of interest.

References

1. Bain, E.C. The nature of solid solutions. *Chem. Met. Eng.* **1923**, *28*, 21–24.
2. Bergman, G.; Shoemaker, D.P. The determination of the crystal structure of the σ phase in the iron–chromium and iron–molybdenum systems. *Acta Cryst.* **1954**, *7*, 857–865. [CrossRef]
3. Boccaccini, L.V.; Giancarli, L.; Janeschitz, G.; Hermsmeyer, S.; Poitevin, Y.; Cardella, A.; Diegele, E. Materials and design of the European DEMO blankets. *J. Nucl. Mater.* **2004**, *148*, 329–333. [CrossRef]
4. Porollo, S.I.; Dvoriashin, A.M.; Vorobyev, A.N.; Yu, V. The microstructure and tensile properties of Fe–Cr alloys after neutron irradiation at 400 C to 5.5–7.1 dPa. *J. Nucl. Mater.* **1998**, *256*, 247–253. [CrossRef]
5. Terentyev, D. Study of radiation effects in FeCr alloys for fusion applications using computer simulations. Ph.D. Thesis, Université Libre de Bruxelles and Belgian Nuclear Research Centre, Bruxelles, Belgium, 2006.
6. Dubiel, S.M.; Costa, B.F.O. Intermediate phases of the α-σ phase transition in the Fe-Cr system. *Phys. Rev. B* **1992**, *47*, 12257. [CrossRef]
7. Kitchingman, W.J. The atomic mechanism of the body-centred cubic to σ-phase transformation. *Acta Cryst. A* **1968**, *24*, 282–286. [CrossRef]
8. Reinhard, L.; Robertson, J.L.; Moss, S.C.; Ice, G.E.; Zschack, P.; Sparks, C.J. Anomalous-X-ray-scattering study of local order in bcc $Fe_{0.53}Cr_{0.47}$. *Phys. Rev. B* **1992**, *45*, 2662. [CrossRef]
9. Turchi, P.E.A.; Reinhard, L.; Stocks, G.M. First-principles study of stability and local order in bcc-based Fe-Cr and Fe-V alloys. *Phys. Rev. B* **1994**, *50*, 15542. [CrossRef]
10. Frattini, R.; Longworth, G.; Matteazzi, P.; Principi, G.; Tiziani, A. Mössbauer studies of surface sigma phase formation in an Fe-45 Cr alloy heated in low partial oxygen pressure. *Scripta Metall.* **1981**, *15*, 873–877. [CrossRef]
11. Ustinovshikov, Y.; Pushkarev, B. Morphology of Fe–Cr alloys. *Mater. Sci. Eng. A* **1998**, *241*, 159–168. [CrossRef]
12. Ustinovshikov, Y.; Pushkarev, B.; Sapegina, I. Phase transformations in alloys of the Fe–V system. *J. Alloys Compd.* **2005**, *398*, 133–138. [CrossRef]
13. Bos, C.; Sommer, F.; Mittemeijer, E.J. Atomistic study on the activation enthalpies for interface mobility and boundary diffusion in an interface-controlled phase transformation. *Philos. Mag.* **2007**, *87*, 2245–2262. [CrossRef]
14. Helbert, C.; Touboul, E.; Perrin, S.; Carraro, L.; Pijolat, M. Stochastic and deterministic models for nucleation and growth in non-isothermal and/or non-isobaric powder transformations. *Chem. Eng. Sci.* **2004**, *59*, 1393–1401. [CrossRef]
15. Blachowski, A.; Cieślak, J.; Dubiel, S.M.; Zukrowski, J. Effect of titanium on the kinetics of the σ-phase formation in a small grain Fe–Cr alloy. *J. Alloys Compd.* **2000**, *308*, 189–192. [CrossRef]
16. International Center for Diffraction Data. *Powder Diffraction File (ICDD-PDF) No 5-708*; ICDD: Square, PA, USA, 1996.
17. Sluiter, M.H.F.; Esfarjani, K.; Kawazoe, Y. Site Occupation Reversal in the Fe−Crσ Phase. *Phys. Rev. Lett.* **1995**, *75*, 3142. [CrossRef] [PubMed]
18. Yakel, H.L. Atom distributions in sigma phases. I. Fe and Cr atom distributions in a binary sigma phase equilibrated at 1063, 1013 and 923 K. *Acta Cryst. B* **1983**, *39*, 20–28. [CrossRef]
19. Korzhavyi, P.A.; Sundman, B.; Selleby, M.; Johansson, B. Atomic, electronic, and magnetic structure of iron-based sigma-phases. *Mater. Res. Soc. Symp. Proc.* **2005**, *842*, 517–522. [CrossRef]

20. Cieślak, J.; Reissner, M.; Dubiel, S.M.; Wernisch, J.; Steiner, W.; (AGH University of Science and Technology, Kraków, Poland). Personal communication, 2007.
21. Al Khoury, W. Etude Structurale par Spectrométrie Mössbauer et Diffraction des Rayons X d'Alliages Fe-Cr à l'Etat Massif et en Couches Minces. Transformation de Phase autour de la Composition Equi-Atomique. Ph.D. Thesis, Poitiers University, Poitiers, France, 2006.
22. Tamura, N.; MacDowell, A.A.; Spolenak, R.; Valek, B.C.; Bravman, J.C.; Brown, W.L.; Celestre, R.S.; Padmore, H.A.; Batterman, B.W.; Patel, J.R. Scanning X-ray microdiffraction with submicrometer white beam for strain/stress and orientation mapping in thin films. *J. Synchrotron Radiat.* **2003**, *10*, 137–143. [CrossRef] [PubMed]
23. Lynch, P.A.; Stevenson, A.W.; Liang, D.; Parry, D.; Wilkins, S.; Tamura, N. A laboratory based system for Laue micro X-ray diffraction. *Rev. Sci. Instrum.* **2007**, *78*, 023904. [CrossRef]
24. Chen, T.H.; Yang, J.R. Effects of solution treatment and continuous cooling on σ-phase precipitation in a 2205 duplex stainless steel. *Mater. Sci. Eng. A* **2001**, *311*, 28–41. [CrossRef]
25. Cieslak, J.; Costa, B.F.O.; Dubiel, S.M.; Le Caer, G. Kinetics of the sigma-to-alpha phase transformation caused by ball milling in near equiatomic Fe−Cr alloys. *Phys. Rev. B* **2006**, *73*, 184123. [CrossRef]
26. Kunz, M.; Tamura, N.; Chen, K.; MacDowell, A.A.; Celestre, R.S.; Church, M.M.; Fakra, S.; Domning, E.E.; Glossinger, J.M.; Plate, D.W.; et al. A dedicated superbend X-ray microdiffraction beamline for materials, geo-, and environmental sciences at the advanced light source. *Rev. Sci. Instrum.* **2009**, *80*, 035108. [CrossRef] [PubMed]
27. Ulrich, O.; Biquard, X.; Bleuet, P.; Geaymond, O.; Gergaud, P.; Micha, J.S.; Robach, O.; Rieutord, F. A new white beam X-ray microdiffraction setup on the BM32 beamline at the European Synchrotron Radiation Facility. *Rev. Sci. Instrum.* **2011**, *82*, 033908. [CrossRef] [PubMed]